Mathematical Modelling and Control

http://www.aimspress.com/journal/mmc

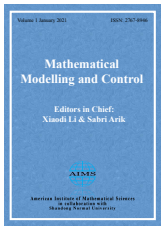

MMC, 4(2): 163–177.
DOI: 10.3934/mmc.2024015
Received: 07 September 2023
Revised: 17 December 2023
Accepted: 29 December 2023
Published: 15 May 2024

*Research article*

# Modeling Rift Valley fever transmission: insights from fractal-fractional dynamics with the Caputo derivative

**Rashid Jan[1,2], Normy Norfiza Abdul Razak[1], Sania Qureshi[3,4,5], Imtiaz Ahmad[6,*] and Salma Bahramand[7]**

[1] Institute of Energy Infrastructure, Department of Civil Engineering, College of Engineering, Universiti Tenaga Nasional, Putrajaya Campus, Jalan Ikram-Uniten, Kajang 43000, Selangor, Malaysia

[2] Mathematics Research Center, Near East University North Cyprus, Mersin 99138, Turkey

[3] Department of Basic Sciences and Related Studies, Mehran University of Engineering and Technology, Jamshoro 76062, Pakistan

[4] Department of Computer Science and Mathematics, Lebanese American University, Beirut, P. O. Box 135053, Lebanon

[5] Department of Mathematics, Near East University, Mersin 99138, Turkey

[6] Institute of Informatics and Computing in Energy, Universiti Tenaga Nasional, Kajang, Selangor, Malaysia

[7] Department of Political Science, Bacha Khan, University Charsadda, Charsadda 24420, Pakistan

* **Correspondence:** Email: imtiazkakakhil@gmail.com.

**Abstract:** The infection caused by Rift Valley fever (RVF) virus is a dangerous vector-borne disease found in humans, domestic, and wild animals. It is transferred through insect vectors to ruminant host and then spread through direct contact of infected animals with their body fluid or organs. In this paper, a fractal-fractional model for the transmission of RVF in the Caputo's sense was presented. We analyzed the model and determined the basic reproduction number through the next-generation matrix technique, indicated by $\mathcal{R}_0$. The global sensitivity technique is used for the sensitivity test of $\mathcal{R}_0$ to find out the most sensitive input-factors to the reproduction parameter $\mathcal{R}_0$. The existence and uniqueness results of the proposed fractal-fractional model were established. Then, we presented the fractal-fractional dynamics of the proposed RVF model through a novel numerical scheme under the fractal-fractional Caputo operator. In the end, the recommended model of RVF was highlighted numerically with the variation of different input parameters of the system. The key factors of the system were highlighted to the policymakers for the control and prevention of the infection.

**Keywords:** Rift Valley fever; fractal-fractional operator; mathematical model; sensitivity analysis; numerical analysis

## 1. Introduction

Infectious diseases pose a significant threat to both the well-being of animals and humans. These diseases result from numerous microorganisms such as bacteria, fungi, parasites, viruses, and other pathogens, causing considerable harm to living organisms. To be more specific, there are direct and indirect routes by which these infections spread to both animals and people. Data is available for diseases such as Hydrophobia, Plague, Measles, Dengue infection, and several others that are transmitted through various methods. One of the notable vector-borne viral zoonoses in Kenya and North Africa is Rift Valley fever virus (RVFV), which is transmitted through mosquitoes. RVFV belongs to the Phlebovirus genus within the Bunyaviridae family. Its presence was first recognized in Kenya during the 1930s [1]. RVFV transmission occurs through diverse routes, including consumption of milk from infected animals, contact with the blood of infected animals, bites from infected vectors, and exposure to the vicinity of infected animals. It is reported

that this viral infection can infect camels, goats, sheep, and cows [2, 3]. The life cycle of RVFV is illustrated in Figure 1 to conceptualize the spread of this infection in the community.

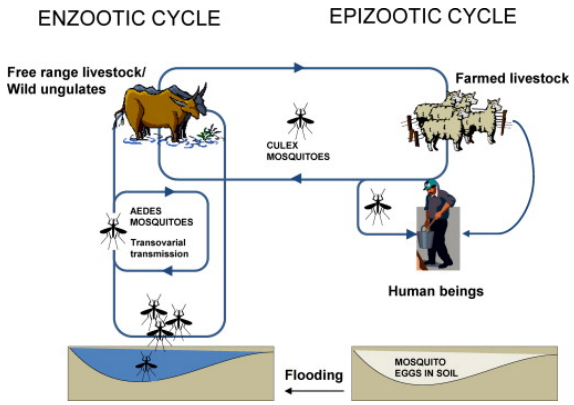


**Figure 1.** Flow chart of transmission cycle of Rift Valley fever virus in the community among hosts and vectors.

The scientific community has introduced multiple dynamic models for examining the transmission dynamics of RVF and providing enhanced recommendations for infection control strategies and medical interventions. Several mathematical models have been explored in previous studies [4, 5] to investigate the transmission mechanisms involved in RVF. Sankhe et al. [6] analyzed the seroprevalence of Crimean-Congo Hemorrhagic fever virus and RVFV in the human population of Senegal during October to November 2020. The study provides insights into the prevalence of these viruses in the region, contributing to our understanding of their potential public health impact. Trabelsi et al. [7] presented serological evidence confirming RVF viral infection in camels imported into Southern Algeria. This suggests potential disease transmission risks and highlights the importance of surveillance and control measures in camel populations in the region.

In another research work, Saul et al. [8] extended the RVF model to include human hosts. Their research involved determining the threshold parameter $\mathcal{R}_0$ for the system and established the local stability of the steady-states. Gitau et al. utilize a gene co-expression network in order to pinpoint significant genes, pathways, and regulatory motifs involved in the development of RVF in Bos taurus [9]. The study provides useful insights into the molecular mechanisms underlying the disease's development and offers potential targets for intervention. Xue et al. [10] introduced a dynamic framework using ordinary differential equations (ODEs) to evaluate the spatial and temporal propagation of RVF. In a related context, Gao et al. [11] formulated a spatially-based three-patch model to conceptualize the transmission of the disease. In their work, they explained the threshold dynamics for each patch and provided visual representations of the dynamic processes. Catre-Sossah et al. [12] gave compelling evidence that both Aedes albopictus and Eretmapodites subsimplicipes play influential roles as competent vectors in the transmission of RVFV in Mayotte, highlighting the importance of understanding their involvement in disease spread. Vaccination is crucial for protecting individuals from infections and reducing the severity of infections, as demonstrated by several studies [13–15].

Numerous vaccines have been created to combat infectious diseases in regions where they are prevalent. However, it is important to acknowledge that not all of these vaccines offer complete effectiveness, and some may be associated with side effects or substantial costs. For instance, concerning RVF, there have been instances of vaccine-related complications in pregnant animals, as noted in a previous study [16]. Ronchi et al. [17] assessed the vaccine's ability to induce an immune response and its safety profile. These findings are crucial for evaluating the vaccine's potential effectiveness in preventing RVF. Morrill et al. [18] reported that the MP-12 vaccine for RVF prompts a rapid and protective immune response in mouse models. This suggests its potential effectiveness as an early intervention against the disease.

Farida et al. [19] introduced a model involving vaccination to examine its impact on reducing losses in ruminant animals. Nevertheless, the full extent of vaccination's influence on the transmission of RVF remains incompletely explored, hindering a comprehensive understanding of this complex system. In this research work, we formulate the dynamics of RVF by incorporating vaccination compartment to more accurately conceptualize the impact of vaccination on the system and to interrogate the system the dynamics of the disease. Moreover, we opt to

visualize the most significant input factors for the control and prevention to lesson the economic burden of RVF on the society. New and more generalized mathematical methods [20–22] and tools are required to examine the dynamics of infection diseases for more reliable and accurate results. Thus, we investigated the dynamics of RVF in the fractal-fractional framework with novel numerical technique.

Remarkable results are obtained through the fractional calculus in different area, such as, mathematics [23, 24], physics [25, 26], economics [27, 28], engineering [29], financial mathematics [30], mathematical biology [31, 32], etc. It has been proved that the modeling of the real-world problem [33, 34] through fractional operators provide accurate results than the ordinary derivatives. To be more specific, the choice of order in fractional operators make it more preeminent than the ordinary operators. Caputo-Fabrizio (CF) [35], Atangana-Baleanu (AB), and Caputo operators are extensively used fractional operators and several efficient results have been achieved in [36, 37]. The models in the framework of fractional operators are more flexible for real data fitting, and the approximation used in the data fitting is used in these models for a future prediction about the problem [38]. For instance, real data has been fitted to several mathematical models in fractional framework with results therein [39, 40]. These models possess the hereditary property and can handle the crossover behavior of intricate models. Among the fractional operators, the Caputo's operator is nonlocal and therefore has more potential abilities to capture complex dynamics of natural phenomena. Furthermore, this approach enables us to incorporate conventional initial and boundary conditions into the problem formulation, as indicated by the findings in [41]. In the framework of Caputo's derivative, it is noteworthy that the derivative of the constant is zero, which enhances the reliability and flexibility of the system for analytical purposes [42]. Motivated by the extra ordinary features, our focus is directed towards the investigation and analysis of RVF dynamics within the framework of a fractal-fractional operator.

The remaining paper is organized as In Section 2, the brief knowledge of fractal-fractional derivative in the Caputo's sense is presented. We introduced a new compartmental model for RVF in the ruminant host in the framework of fractal-fractional Caputo derivative in Section 3. Furthermore, we investigate the proposed model and compute the reproduction parameter of the system, indicated by $\mathcal{R}_0$. Global sensitivity analysis and some numerical results are carried out for $\mathcal{R}_0$ to investigate the importance of parameters in the structure of $\mathcal{R}_0$. In Section 4, we introduced a new numerical scheme for the proposed fractal-fractional model, and establish the existence and uniqueness results for the newly developed scheme. In the end, we visualized the proposed fractal-fractional model of RVF through the novel numerical scheme with different values of fractals and fractional order in Section 5. Concluding remarks of the overall research are given in the final section of this work.

## 2. Concepts of fractal-fractional operators

In this section, we represent a brief summary of fractal-fractional calculus associated with some operators mentioned in [43], which will be helpful for the analysis of our model in the upcoming sections.

**Definition 2.1.** *Let us assume a continues and differentiable function $y(t)$ on the interval $(c, e)$ with order $\vartheta$; then, the Riemann-Liouville fractal-fractional derivative of $y(t)$ with the power kernel of order $\varrho$ is defined in the following way*

$$^{FFP}D^{\varrho,\vartheta}_{0,t}(y(t)) = \frac{1}{\Gamma(l-\varrho)}\frac{d}{dt^{\vartheta}}\int_0^t (t-r)^{l-\varrho-1}y(r)dr,$$

*where $l-1 < \varrho, \vartheta, l \in \mathbf{N}$ such that $\vartheta \leq l$ and*

$$\frac{dy(r)}{dr^{\vartheta}} = \lim_{t\to r}\frac{y(t)-y(r)}{t^{\vartheta}-r^{\vartheta}}.$$

**Definition 2.2.** *Let us assume a continues and differentiable function $y(t)$ on the interval $(c, e)$ with order $\vartheta$; then, the Riemann-Liouville fractal-fractional derivative of $y(t)$ with exponentially decaying kernel of order $\varrho$ is defined in the following way*

$$^{FFE}D^{\varrho,\vartheta}_{0,t}(y(t)) = \frac{M(\varrho)}{(1-\varrho)}\frac{d}{dt^{\vartheta}}\int_0^t exp\Big[-\frac{\varrho}{1-\varrho}(t-r)\Big]y(r)dr,$$

*where $M(0) = M(1) = 1, \varrho > 0, \vartheta \leq l \in \mathbf{N}$.*

**Definition 2.3.** *Let us assume a continues and differentiable function $y(t)$ on the interval $(c, e)$ with order $\vartheta$; then, the*

*Riemann-Liouville fractal-fractional derivative of $y(t)$ with a kernel of generalized Mittag-Leffler form of order $\varrho$ is defined in the following way*

$$^{FFM}D^{\varrho,\vartheta}_{0,t}(y(t)) = \frac{AB(\varrho)}{1-\varrho}\frac{d}{dt^{\vartheta}}\int_0^t E_{\varrho}\Big[-\frac{\varrho}{1-\varrho}(t-r)^{\varrho}\Big]y(r)dr,$$

*where*

$$AB(\varrho) = 1-\varrho+\frac{\varrho}{\Gamma(\varrho)},\ \ \varrho>0$$

*and $\vartheta \le l \in \mathbf{N}$.*

**Definition 2.4.** *Let us assume a continues and differentiable function $y(t)$ on the interval $(c,e)$ with order $\vartheta$; then, the fractal-fractional integral of $y(t)$ with a kernel of the power law form of order $\varrho$ is defined in the following way*

$$^{FFP}J^{\varrho}_{0,t}(y(t)) = \frac{\vartheta}{\Gamma(\varrho)}\int_0^t (t-r)^{\varrho-1}r^{\vartheta-1}y(r)dr.$$

**Definition 2.5.** *Let us assume a continues and differentiable function $y(t)$ on the interval $(c,e)$ with order $\vartheta$; then, the fractal-fractional integral of $y(t)$ with a kernel of exponential decaying form of order $\varrho$ is introduced in the following way*

$$^{FFE}J^{\varrho}_{0,t}(y(t)) = \frac{\varrho\vartheta}{M(\varrho)}\int_0^t r^{\varrho-1}y(r)dr + \frac{\vartheta(1-\varrho)t^{\vartheta-1}y(t)}{M(\varrho)}.$$

**Definition 2.6.** *Let us assume a continues and differentiable function $y(t)$ on the interval $(c,e)$ with order $\vartheta$; then, the fractal-fractional integral of $y(t)$ with a kernel of generalized Mittag-Leffler form of order $\varrho$ is introduced in the following way*

$$^{FFM}J^{\varrho,\vartheta}_{0,t}(y(t)) = \frac{\varrho\vartheta}{AB(\varrho)}\int_0^t r^{\vartheta-1}(t-r)^{\varrho-1}y(r)dr + \frac{\vartheta(1-\varrho)t^{\vartheta-1}y(t)}{AB(\varrho)}.$$

## 3. Model formulation

In the formulation of the model, the complete vector population size, denoted as $M$ representing female mosquitoes, is divided into two groups: Those that are susceptible, referred to as $(S_m)$, and those that are infected, represented as $(I_m)$. Similarly, the overall ruminant population, denoted as $N_r$, is classified into four compartments: susceptible individuals, denoted as $(S_r)$; individuals who have been vaccinated, denoted as $(V_r)$; infected individuals, denoted as $(I_r)$; and individuals who have recovered from the infection, denoted as $(R_r)$. The rate of recruitment for the ruminant population and female mosquitoes is represented as $\Pi_r$ and $\Pi_m$, respectively. We use $d_r$ to signify the inherent mortality rate of ruminants, and likewise, $d_m$ denotes the natural mortality rate of mosquitoes. Additionally, $\delta$ corresponds to the mortality rate caused by the disease, and $\gamma$ signifies the rate of recovery. It is assumed that a proportion $v$ of the susceptible population changes from the unvaccinated category after vaccination to the vaccinated category. The $\beta_r$ and $\beta_m$, respectively, stand for the probability of transmission from the host to the vector and from the vector to the host. The effectiveness of vaccination is indicated by the parameter $\alpha$, and the rate at which mosquitoes bite their hosts is symbolized by $b$. Moreover, we assumed that a fraction $\rho$ of the vaccinated class moves to the recovered class after recovery. The dynamics of RVF transmission are described by

$$\begin{cases} \frac{dS_r}{dt} = \Pi_r - b\beta_r S_r I_m - vS_r - d_r S_r, \\ \frac{dV_r}{dt} = vS_r - (1-\alpha)b\beta_r V_r I_m - \rho V_r - d_r V_r, \\ \frac{dI_r}{dt} = b\beta_r S_r I_m + (1-\alpha)b\beta_r V_r I_m - (d_r+\gamma+\delta)I_r, \\ \frac{dR_r}{dt} = \rho V_r + \gamma I_r - d_r R_r, \\ \frac{dS_m}{dt} = \Pi_m - b\beta_m S_m I_r - d_m S_m, \\ \frac{dI_m}{dt} = b\beta_m S_m I_r - d_m I_m, \end{cases} \tag{3.1}$$

with positive initial state values given by $S_m(0), I_m(0), S_r(0), V_r(0), I_r(0), R_r(0)$.

The applications of fractal fractional derivatives span diverse areas, including image analysis, financial modeling, and the study of complex biological systems. By incorporating the concept of fractality into fractional calculus, researchers and scientists can gain deeper insights into the inherent complexity of natural phenomena, leading to more accurate modeling and predictions in a wide range of disciplines [44]. The above RVF model in fractal-fractional Caputo derivative form can be depicted as follows

$$\begin{cases} ^{FF}D^{\wp,\vartheta}_{0,t}(S_r) = \Pi_r - b\beta_r S_r I_m - vS_r - d_r S_r, \\ ^{FF}D^{\wp,\vartheta}_{0,t}(V_r) = vS_r - (1-\alpha)b\beta_r V_r I_m - \rho V_r - d_r V_r, \\ ^{FF}D^{\wp,\vartheta}_{0,t}(I_r) = b\beta_r S_r I_m + (1-\alpha)b\beta_r V_r I_m - (d_r+\gamma+\delta)I_r, \\ ^{FF}D^{\wp,\vartheta}_{0,t}(R_r) = \rho V_r + \gamma I_r - d_r R_r, \\ ^{FF}D^{\wp,\vartheta}_{0,t}(S_m) = \Pi_m - b\beta_m S_m I_r - d_m S_m, \\ ^{FF}D^{\wp,\vartheta}_{0,t}(I_m) = b\beta_m S_m I_r - d_m I_m, \end{cases} \tag{3.2}$$

where $^{FF}D^{\wp,\vartheta}_{0,t}$ indicates the Caputo fractal-fractional derivative with fractal and fractional orders $\wp$ and $\vartheta$,

respectively. In the upcoming subsection, we will examine our recommended fractal-fractional model of RVF.

### 3.1. Analysis of the model

In examining the Caputo model with fractal-fractional characteristics (3.2), our initial emphasis is on analyzing the disease-free equilibrium state of the system. To determine this equilibrium state, our first step involves examining the following conditions for steady-state (3.2)

$$ {}^{FF}D_{0,t}^{\varphi,\vartheta}(S_r(t)) = 0, \quad {}^{FF}D_{0,t}^{\varphi,\vartheta}(V_r(t)) = 0, \quad {}^{FF}D_{0,t}^{\varphi,\vartheta}(I_r(t)) = 0 $$

and

$$ {}^{FF}D_{0,t}^{\varphi,\vartheta}(R_r(t)) = 0, \quad {}^{FF}D_{0,t}^{\varphi,\vartheta}(S_m(t)) = 0, \quad {}^{FF}D_{0,t}^{\varphi,\vartheta}(I_m(t)) = 0, $$

and obtain the steady-state as

$$ \begin{cases} 0 = \Pi_r - b\beta_r S_r I_m - vS_r - d_r S_r, \\ 0 = vS_r - (1-\alpha)b\beta_r V_r I_m - \rho V_r - d_r V_r, \\ 0 = b\beta_r S_r I_m + (1-\alpha)b\beta_r V_r I_m - (d_r + \gamma + \delta) I_r, \\ 0 = \rho V_r + \gamma I_r - d_r R_r, \\ 0 = \Pi_m - b\beta_m S_m I_r - d_m S_m, \\ 0 = b\beta_m S_m I_r - d_m I_m. \end{cases} \tag{3.3} $$

Next, we take the above system (3.3) without infection and get the following disease-free equilibrium

$$ E_0 = \left(\frac{\Pi_r}{v + d_r}, \frac{v\Pi_r}{(v + d_r)(\rho + d_r)}, 0, \frac{\rho v \Pi_r}{d_r(v + d_r)(\rho + d_r)}, \frac{\Pi_m}{d_m}, 0\right). $$

Furthermore, we will used the approach outlined in previous works [45] to compute the basic reproduction number, which is determined as follows

$$ \mathcal{F} = \begin{bmatrix} b\beta_r S_r I_m + (1-\alpha)b\beta_r V_r I_m \\ b\beta_m S_m I_r \end{bmatrix} $$

and

$$ \mathcal{V} = \begin{bmatrix} (d_r + \gamma + \delta) I_r \\ d_m I_m \end{bmatrix}, $$

due to the presence of two infected compartments within the system, this consequently suggests

$$ F = \begin{bmatrix} 0 & b\beta_r S_r^0 + (1-\alpha)b\beta_r V_r^0 \\ b\beta_m S_m^0 & 0 \end{bmatrix} $$

and

$$ \mathrm{V} = \begin{bmatrix} (d_r + \gamma + \delta) & 0 \\ 0 & d_m \end{bmatrix}, $$

which gives

$$ FV^{-1} = \begin{bmatrix} 0 & \left(\frac{b\beta_r S_r^0 + (1-\alpha)b\beta_r V_r^0}{d_m}\right) \\ \frac{b\beta_m S_m^0}{(d_r+\gamma+\delta)} & 0 \end{bmatrix}. $$

We write $\mathcal{R}$, for the fractal-fractional RVF model's fundamental reproduction number. It is derived through the utilization of the next-generation matrix, which is represented as

$$ \rho(FV^{-1}) = \sqrt{\frac{b\beta_m S_m^0}{(d_r + \gamma + \delta)}\left(\frac{b\beta_r S_r^0 + (1-\alpha)b\beta_r V_r^0}{d_m}\right)} $$

and

$$ \mathcal{R}_0 = \sqrt{\frac{b\beta_m S_m^0}{d_m}\left(\frac{b\beta_r S_r^0 + (1-\alpha)b\beta_r V_r^0}{(d_r + \gamma + \delta)}\right)}. $$

In this work, we focussed on the dynamical behavior of the system to investigate the solution pathways in different scenarios. However, the stability (Ulam-Hyers stability) and other aspects of the model will be considered in the future work [46, 47].

### 3.2. Sensitivity analysis and numerical results

Sensitivity analysis is used to show the influence of input values on the output of several dynamical systems arising from natural phenomena. It is well known that the local sensitivity analysis is not always suitable for intricate systems and does not provide enough information about the complexity of the system parameters. Therefore in this work, we focus on the global sensitivity analysis to investigate our proposed system and to detect the critical values effecting the output of the system. The partial rank correlation coefficient (PRCC) method is most reliable and efficient method to analyze the sensitivity of a system and provide better information about the critical factors involved in the formulation of the dynamical system [48]. In this analysis, an input parameter with the highest PRCC value and the smallest p-value is considered to be the most critical factor of the system.

We used PRCC method [48] for sensitivity analysis of the basic reproduction number $\mathcal{R}_0$. In our sensitivity analysis, we examined ten input parameters from Table 1 to assess their impact on the output of $\mathcal{R}_0$. We have compiled a list

of the corresponding PRCC values and their associated p-values as determined by the PRCC significance test. The parameters $b$ and $d_m$ demonstrate the significant influence, as seen by their PRCC values of 0.8790, -0.7919, respectively, as shown in Figure 2 and Table 2. Subsequently, the parameters $\beta_r$ and $\beta_m$ also exert significant effects on the basic reproduction number, with PRCC values of 0.6727 and 0.5433, respectively. This suggests that implementing control measures to reduce the value of $b$ and increase the value of $d_m$ can effectively mitigate the impact of RVF.

**Table 1.** Explanation detailing the input parameters and their associated numerical values for the RVF model.

| Symbol | Interpretation | Values | Reference |
|---|---|---|---|
| $d_r$ | The natural mortality rate of ruminant | 0.000481 | [49] |
| $v$ | The susceptibility of ruminants to $V_r$ as a vaccination factor | 0.7 | Assumed |
| $\gamma$ | Rate of recovery among ruminants that are infected | 0.0875 | [19] |
| $\vartheta$ | Fractional order | Assumed | Assumed |
| $\varphi$ | Fractal order | Assumed | Assumed |
| $b$ | Vector biting rate | 0.701 | [50] |
| $\beta_r$ | Transfer of the virus from mosquitoes to vulnerable ruminant | 0.14 | [51] |
| $\alpha$ | Vaccine effectiveness or vaccine potency | 0.6 | Assumed |
| $\rho$ | Recovery of ruminant hosts through vaccination | 0.5 | Assumed |
| $\beta_m$ | Transfer of the virus from ruminants to vulnerable mosquitoes | 0.35 | [51] |
| $d_m$ | The natural mortality rate of mosquitoes | 0.0166 | [52] |
| $\Pi_r$ | Rate of recruitment of hosts from the ruminant category | Variable | Assumed |
| $\Pi_m$ | Rate of recruitment of mosquito vectors | Variable | Assumed |
| $\delta$ | Mortality rate attributed to the disease | 0.0214 | Assumed |

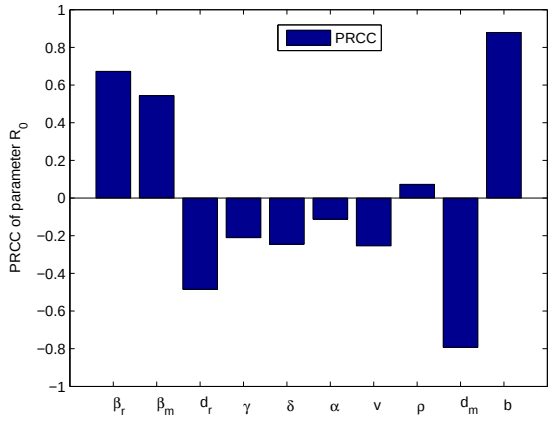


**Figure 2.** Conducting a sensitivity analysis on input parameters affecting $\mathcal{R}_0$ and examining their correlation with PRCC results.

**Table 2.** Sensitivity findings for $\mathcal{R}_0$ using PRCC and the associated statistical significance levels.

| Parameter | Interpretation | PRCC values | p values |
|---|---|---|---|
| $\beta_r$ | Transfer from mosquitoes to vulnerable ruminants | +0.6727 | 0.0000 |
| $\beta_m$ | Transmission from ruminants to susceptible mosquitoes | +0.5433 | 0.0000 |
| $d_r$ | Host ruminants natural death rate | -0.4841 | 0.0000 |
| $\gamma$ | Recovery rate of host individuals | -0.2101 | 0.0000 |
| $\delta$ | Disease induced death rate | -0.2444 | 0.0000 |
| $\alpha$ | Efficacy of vaccine or strength of vaccine | -0.1119 | 0.0004 |
| $v$ | Vaccinated fraction of susceptible ruminants | -0.2541 | 0.0000 |
| $\rho$ | Recovery rate through vaccination | +0.0726 | 0.0223 |
| $d_m$ | Vector mosquitoes natural death rate | -0.7919 | 0.0000 |
| $b$ | Vector mosquitoes biting rate | +0.8790 | 0.0000 |

To delve into details, adjusting these factors allows us to notably reduce, and perhaps eradicate, the emergence of new RVF cases. Furthermore, we illustrated the variation of the threshold parameter $\mathcal{R}_0$ by varying different parameters numerically, as depicted in Figures 3 and 4.

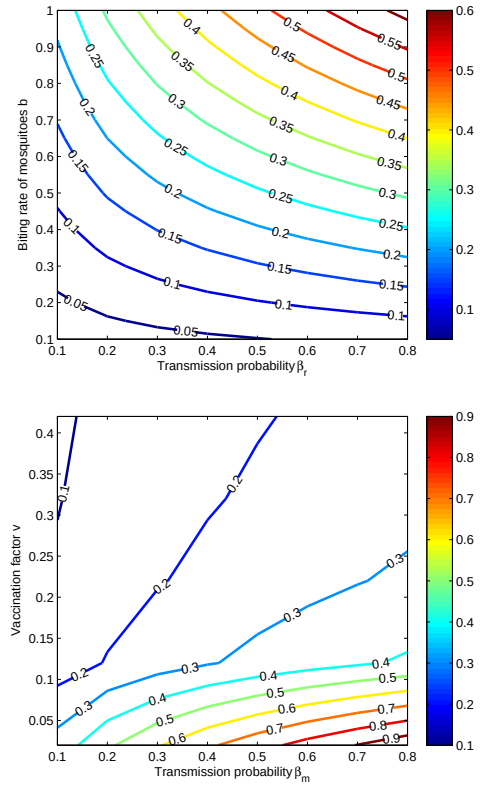


**Figure 3.** Visualization of the fundamental reproduction number $\mathcal{R}_0$ (a) by varying the biting rate $b$ and transmission probability $\beta_r$, and in (b) by altering the vaccination rate $v$ and transmission probability $\beta_m$.

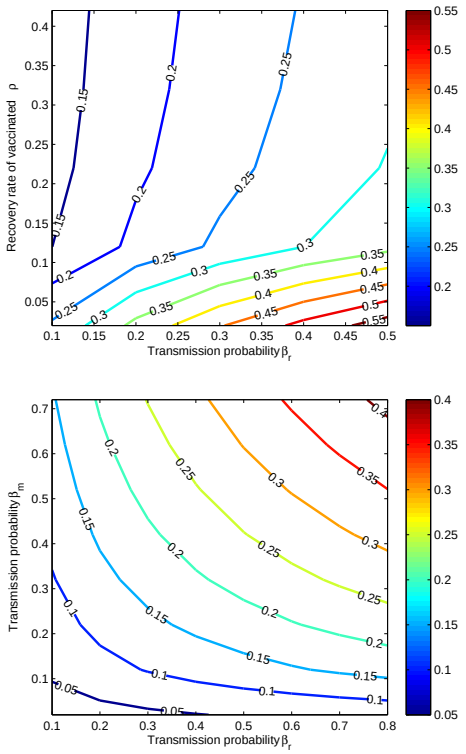


**Figure 4.** Illustration of basic reproduction number $\mathcal{R}_0$ (a) considering changes in the transmission probability parameters $\beta_r$ and $\rho$, (b) and examining variations in transmission probabilities $\beta_r$ and $\beta_m$.

## 4. New approach for fractal-fractional Caputo system

In this section, we will propose a novel numerical technique for the fractal-fractional Caputo (FFC) derivative to obtain the numerical results for our model (3.2). We first convert FFC system to Volteera, then the system FFC in the sense of Riemann-Liouville can be represented in the following form

$$\frac{1}{\Gamma(1-\wp)}\frac{d}{dt}\int_0^t (t-\vartheta)^{\wp} f(\vartheta)d\vartheta \frac{1}{\vartheta t^{\vartheta-1}}, \tag{4.1}$$

then, we have the following:

$$\begin{aligned}
{}^{RL}D^{\wp}_{0,t}(S_r) &= \vartheta t^{\vartheta-1}(\Pi_r - b\beta_r S_r I_m - vS_r - d_r S_r),\\
{}^{RL}D^{\wp}_{0,t}(V_r) &= \vartheta t^{\vartheta-1}(vS_r - (1-\alpha)b\beta_r V_r I_m - \rho V_r - d_r V_r),\\
{}^{RL}D^{\wp}_{0,t}(I_r) &= \vartheta t^{\vartheta-1}(b\beta_r S_r I_m + (1-\alpha)b\beta_r V_r I_m - (d_r+\gamma+\delta)I_r),\\
{}^{RL}D^{\wp}_{0,t}(R_r) &= \vartheta t^{\vartheta-1}(\rho V_r + \gamma I_r - d_r R_r),\\
{}^{RL}D^{\wp}_{0,t}(S_m) &= \vartheta t^{\vartheta-1}(\Pi_m - b\beta_m S_m I_r - d_m S_m),\\
{}^{RL}D^{\wp}_{0,t}(I_m) &= \vartheta t^{\vartheta-1}(b\beta_m S_m I_r - d_m I_m),
\end{aligned} \tag{4.2}$$

we convert Riemann-Liouville derivative to Caputo derivative in to make it flexible for the initial conditions. In the next step, we apply the fractional integral and get the below

$$\begin{aligned}
S_r(t) &= S_r(0) + \frac{\vartheta}{\Gamma(\wp)}\int_0^t \chi^{\vartheta-1}(t-\chi)^{\wp-1} g_1(S_r,V_r,I_r,R_r,S_m,I_m,\chi)d\chi,\\
V_r(t) &= V_r(0) + \frac{\vartheta}{\Gamma(\wp)}\int_0^t \chi^{\vartheta-1}(t-\chi)^{\wp-1} g_2(S_r,V_r,I_r,R_r,S_m,I_m,\chi)d\chi,\\
I_r(t) &= I_r(0) + \frac{\vartheta}{\Gamma(\wp)}\int_0^t \chi^{\vartheta-1}(t-\chi)^{\wp-1} g_3(S_r,V_r,I_r,R_r,S_m,I_m,\chi)d\chi,\\
R_r(t) &= R_r(0) + \frac{\vartheta}{\Gamma(\wp)}\int_0^t \chi^{\vartheta-1}(t-\chi)^{\wp-1} g_4(S_r,V_r,I_r,R_r,S_m,I_m,\chi)d\chi,\\
S_m(t) &= S_m(0) + \frac{\vartheta}{\Gamma(\wp)}\int_0^t \chi^{\vartheta-1}(t-\chi)^{\wp-1} g_5(S_r,V_r,I_r,R_r,S_m,I_m,\chi)d\chi,\\
I_m(t) &= I_m(0) + \frac{\vartheta}{\Gamma(\wp)}\int_0^t \chi^{\vartheta-1}(t-\chi)^{\wp-1} g_6(S_r,V_r,I_r,R_r,S_m,I_m,\chi)d\chi,
\end{aligned} \tag{4.3}$$

where

$$\begin{aligned}
g_1(S_r,V_r,I_r,R_r,S_m,I_m,\chi) &= \Pi_r - b\beta_r S_r I_m - vS_r - d_r S_r,\\
g_2(S_r,V_r,I_r,R_r,S_m,I_m,\chi) &= vS_r - (1-\alpha)b\beta_r V_r I_m - \rho V_r - d_r V_r,\\
g_3(S_r,V_r,I_r,R_r,S_m,I_m,\chi) &= b\beta_r S_r I_m + (1-\alpha)b\beta_r V_r I_m\\
&\quad - (d_r+\gamma+\delta)I_r,\\
g_4(S_r,V_r,I_r,R_r,S_m,I_m,\chi) &= \rho V_r + \gamma I_r - d_r R_r,\\
g_5(S_r,V_r,I_r,R_r,S_m,I_m,\chi) &= \Pi_m - b\beta_m S_m I_r - d_m S_m,\\
g_6(S_r,V_r,I_r,R_r,S_m,I_m,\chi) &= b\beta_m S_m I_r - d_m I_m.
\end{aligned}$$

Using a novel idea at the time $t_{m+1}$, the model become as

$$\begin{aligned}
S_r(t) &= S_r(0) + \frac{\vartheta}{\Gamma(\wp)}\int_0^t \chi^{\vartheta-1}(t_{n+1}-\chi)^{\wp-1} g_1 \qquad (4.4)\\
&\quad (S_r,V_r,I_r,R_r,S_m,I_m,\chi)d\chi,\\
V_r(t) &= V_r(0) + \frac{\vartheta}{\Gamma(\wp)}\int_0^t \chi^{\vartheta-1}(t_{n+1}-\chi)^{\wp-1} g_2 \qquad (4.5)\\
&\quad (S_r,V_r,I_r,R_r,S_m,I_m,\chi)d\chi,\\
I_r(t) &= I_r(0) + \frac{\vartheta}{\Gamma(\wp)}\int_0^t \chi^{\vartheta-1}(t_{n+1}-\chi)^{\wp-1} g_3 \qquad (4.6)\\
&\quad (S_r,V_r,I_r,R_r,S_m,I_m,\chi)d\chi,\\
R_r(t) &= R_r(0) + \frac{\vartheta}{\Gamma(\wp)}\int_0^t \chi^{\vartheta-1}(t_{n+1}-\chi)^{\wp-1} g_4 \qquad (4.7)\\
&\quad (S_r,V_r,I_r,R_r,S_m,I_m,\chi)d\chi,\\
S_m(t) &= S_m(0) + \frac{\vartheta}{\Gamma(\wp)}\int_0^t \chi^{\vartheta-1}(t_{n+1}-\chi)^{\wp-1} g_5 \qquad (4.8)\\
&\quad (S_r,V_r,I_r,R_r,S_m,I_m,\chi)d\chi,\\
I_m(t) &= I_m(0) + \frac{\vartheta}{\Gamma(\wp)}\int_0^t \chi^{\vartheta-1}(t_{n+1}-\chi)^{\wp-1} g_6 \qquad (4.9)\\
&\quad (S_r,V_r,I_r,R_r,S_m,I_m,\chi)d\chi.
\end{aligned}$$

We get the following after approximation the above expression (4.4), we obtain

$$S_r^{m+1} = S_r^0 + \frac{\vartheta}{\Gamma(\wp)} \sum_{j=0}^{m} \int_{t_j}^{t_{j+1}} \chi^{\vartheta-1}(t_{m+1}-\chi)^{\wp-1} g_1 \quad (4.10)$$
$$(S_r, V_r, I_r, R_r, S_m, I_m, \chi)d\chi,$$

$$V_r^{m+1} = V_r^0 + \frac{\vartheta}{\Gamma(\wp)} \sum_{j=0}^{m} \int_{t_j}^{t_{j+1}} \chi^{\vartheta-1}(t_{m+1}-\chi)^{\wp-1} g_2 \quad (4.11)$$
$$(S_r, V_r, I_r, R_r, S_m, I_m, \chi)d\chi,$$

$$I_r^{m+1} = I_r^0 + \frac{\vartheta}{\Gamma(\wp)} \sum_{j=0}^{m} \int_{t_j}^{t_{j+1}} \chi^{\vartheta-1}(t_{m+1}-\chi)^{\wp-1} g_3 \quad (4.12)$$
$$(S_r, V_r, I_r, R_r, S_m, I_m, \chi)d\chi,$$

$$R_r^{m+1} = R_r^0 + \frac{\vartheta}{\Gamma(\wp)} \sum_{j=0}^{m} \int_{t_j}^{t_{j+1}} \chi^{\vartheta-1}(t_{m+1}-\chi)^{\wp-1} g_4 \quad (4.13)$$
$$(S_r, V_r, I_r, R_r, S_m, I_m, \chi)d\chi,$$

$$S_m^{m+1} = S_m^0 + \frac{\vartheta}{\Gamma(\wp)} \sum_{j=0}^{m} \int_{t_j}^{t_{j+1}} \chi^{\vartheta-1}(t_{m+1}-\chi)^{\wp-1} g_5 \quad (4.14)$$
$$(S_r, V_r, I_r, R_r, S_m, I_m, \chi)d\chi,$$

$$I_m^{m+1} = I_m^0 + \frac{\vartheta}{\Gamma(\wp)} \sum_{j=0}^{m} \int_{t_j}^{t_{j+1}} \chi^{\vartheta-1}(t_{m+1}-\chi)^{\wp-1} g_6 \quad (4.15)$$
$$(S_r, V_r, I_r, R_r, S_m, I_m, \chi)d\chi.$$

Furthermore, the Lagrangian piece-wise interpolation is used to approximate the function $\chi^{\vartheta-1} g_1(S_r, V_r, I_r, R_r, S_m, I_m, \chi)$ on the interval $[t_j, t_{j+1}]$, then we have

$$\begin{aligned}
P_j(\chi) &= \frac{\chi - t_{j-1}}{t_j - t_{j-1}} t_j^{\vartheta-1} g_1(S_r^j, V_r^j, I_r^j, R_r^j, S_m^j, I_m^j, t_j) \\
&\quad - \frac{\chi - t_j}{t_j - t_{j-1}} t_{j-1}^{\vartheta-1} g_1(S_r^{j-1}, V_r^{j-1}, I_r^{j-1}, R_r^{j-1}, S_m^{j-1}, I_m^{j-1}, t_{j-1}), \\
Q_j(\chi) &= \frac{\chi - t_{j-1}}{t_j - t_{j-1}} t_j^{\vartheta-1} g_2(S_r^j, V_r^j, I_r^j, R_r^j, S_m^j, I_m^j, t_j) \\
&\quad - \frac{\chi - t_j}{t_j - t_{j-1}} t_{j-1}^{\vartheta-1} g_2(S_r^{j-1}, V_r^{j-1}, I_r^{j-1}, R_r^{j-1}, S_m^{j-1}, I_m^{j-1}, t_{j-1}), \\
R_j(\chi) &= \frac{\chi - t_{j-1}}{t_j - t_{j-1}} t_j^{\vartheta-1} g_3(S_r^j, V_r^j, I_r^j, R_r^j, S_m^j, I_m^j, t_j) \\
&\quad - \frac{\chi - t_j}{t_j - t_{j-1}} t_{j-1}^{\vartheta-1} g_3(S_r^{j-1}, V_r^{j-1}, I_r^{j-1}, R_r^{j-1}, S_m^{j-1}, I_m^{j-1}, t_{j-1}), \\
S_j(\chi) &= \frac{\chi - t_{j-1}}{t_j - t_{j-1}} t_j^{\vartheta-1} g_4(S_r^j, V_r^j, I_r^j, R_r^j, S_m^j, I_m^j, t_j) \\
&\quad - \frac{\chi - t_j}{t_j - t_{j-1}} t_{j-1}^{\vartheta-1} g_4(S_r^{j-1}, V_r^{j-1}, I_r^{j-1}, R_r^{j-1}, S_m^{j-1}, I_m^{j-1}, t_{j-1}), \\
T_j(\chi) &= \frac{\chi - t_{j-1}}{t_j - t_{j-1}} t_j^{\vartheta-1} g_5(S_r^j, V_r^j, I_r^j, R_r^j, S_m^j, I_m^j, t_j) \\
&\quad - \frac{\chi - t_j}{t_j - t_{j-1}} t_{j-1}^{\vartheta-1} g_5(S_r^{j-1}, V_r^{j-1}, I_r^{j-1}, R_r^{j-1}, S_m^{j-1}, I_m^{j-1}, t_{j-1}),
\end{aligned} \quad (4.16)$$

$$\begin{aligned}
U_j(\chi) &= \frac{\chi - t_{j-1}}{t_j - t_{j-1}} t_j^{\vartheta-1} g_6(S_r^j, V_r^j, I_r^j, R_r^j, S_m^j, I_m^j, t_j) \\
&\quad - \frac{\chi - t_j}{t_j - t_{j-1}} t_{j-1}^{\vartheta-1} g_6(S_r^{j-1}, V_r^{j-1}, I_r^{j-1}, R_r^{j-1}, S_m^{j-1}, I_m^{j-1}, t_{j-1}).
\end{aligned}$$

So, the following is obtained:

$$\begin{aligned}
S_r^{m+1} &= S_r^0 + \frac{\vartheta}{\Gamma(\wp)} \sum_{j=0}^{m} \int_{t_j}^{t_{j+1}} \chi^{\vartheta-1}(t_{m+1}-\chi)^{\wp-1} P_j(\chi)d\chi, \\
V_r^{m+1} &= V_r^0 + \frac{\vartheta}{\Gamma(\wp)} \sum_{j=0}^{m} \int_{t_j}^{t_{j+1}} \chi^{\vartheta-1}(t_{m+1}-\chi)^{\wp-1} Q_j(\chi)d\chi, \\
I_r^{m+1} &= I_r^0 + \frac{\vartheta}{\Gamma(\wp)} \sum_{j=0}^{m} \int_{t_j}^{t_{j+1}} \chi^{\vartheta-1}(t_{m+1}-\chi)^{\wp-1} R_j(\chi)d\chi, \\
R_r^{m+1} &= R_r^0 + \frac{\vartheta}{\Gamma(\wp)} \sum_{j=0}^{m} \int_{t_j}^{t_{j+1}} \chi^{\vartheta-1}(t_{m+1}-\chi)^{\wp-1} S_j(\chi)d\chi, \\
S_m^{m+1} &= S_m^0 + \frac{\vartheta}{\Gamma(\wp)} \sum_{j=0}^{m} \int_{t_j}^{t_{j+1}} \chi^{\vartheta-1}(t_{m+1}-\chi)^{\wp-1} T_j(\chi)d\chi, \\
I_r^{m+1} &= I_r^0 + \frac{\vartheta}{\Gamma(\wp)} \sum_{j=0}^{m} \int_{t_j}^{t_{j+1}} \chi^{\vartheta-1}(t_{m+1}-\chi)^{\wp-1} U_j(\chi)d\chi.
\end{aligned} \quad (4.17)$$

The solution of the above Eq (4.17) lead finally to the below equations:

$$\begin{aligned}
S_r^{m+1} &= S_r^0 + \frac{\vartheta h^\wp}{\Gamma(\wp+2)} \sum_{j=0}^{m} \Big[ t_j^{\vartheta-1} g_1(S_r^j, V_r^j, I_r^j, R_r^j, S_m^j, I_m^j, t_j) \\
&\quad \times \Big[ (m+1-j)^\wp (m-j+2+\wp) - (m-j)^\wp (m-j \\
&\quad + 2 + 2\wp) \Big] - t_{j-1}^{\vartheta-1} g_1(S_r^{j-1}, V_r^{j-1}, I_r^{j-1}, R_r^{j-1}, S_m^{j-1}, I_m^{j-1}, \\
&\quad t_{j-1}) \times \Big( (m-j+1)^{\wp+1} - (m-j)^\wp (m-j+1+\wp) \Big) \Big], \\
V_r^{m+1} &= V_r^0 + \frac{\vartheta h^\wp}{\Gamma(\wp+2)} \sum_{j=0}^{m} \Big[ t_j^{\vartheta-1} g_2(S_r^j, V_r^j, I_r^j, R_r^j, S_m^j, I_m^j, t_j) \\
&\quad \times \Big[ (m+1-j)^\wp (m-j+2+\wp) - (m-j)^\wp (m-j \\
&\quad + 2 + 2\wp) \Big] - t_{j-1}^{\vartheta-1} g_2(S_r^{j-1}, V_r^{j-1}, I_r^{j-1}, R_r^{j-1}, S_m^{j-1}, I_m^{j-1}, \\
&\quad t_{j-1}) \times \Big( (m-j+1)^{\wp+1} - (m-j)^\wp (m-j+1+\wp) \Big) \Big], \\
I_r^{m+1} &= I_r^0 + \frac{\vartheta h^\wp}{\Gamma(\wp+2)} \sum_{j=0}^{m} \Big[ t_j^{\vartheta-1} g_3(S_r^j, V_r^j, I_r^j, R_r^j, S_m^j, I_m^j, t_j) \\
&\quad \times \Big[ (m+1-j)^\wp (m-j+2+\wp) - (m-j)^\wp (m-j \\
&\quad + 2 + 2\wp) \Big] - t_{j-1}^{\vartheta-1} g_3(S_r^{j-1}, V_r^{j-1}, I_r^{j-1}, R_r^{j-1}, S_m^{j-1}, I_m^{j-1}, \\
&\quad t_{j-1}) \times \Big( (m-j+1)^{\wp+1} - (m-j)^\wp (m-j+1+\wp) \Big) \Big], \\
R_r^{m+1} &= R_r^0 + \frac{\vartheta h^\wp}{\Gamma(\wp+2)} \sum_{j=0}^{m} \Big[ t_j^{\vartheta-1} g_4(S_r^j, V_r^j, I_r^j, R_r^j, S_m^j, I_m^j, t_j) \\
&\quad \times \Big[ (m+1-j)^\wp (m-j+2+\wp) - (m-j)^\wp (m-j+2 \\
&\quad + 2\wp) \Big] - t_{j-1}^{\vartheta-1} g_4(S_r^{j-1}, V_r^{j-1}, I_r^{j-1}, R_r^{j-1}, S_m^{j-1}, I_m^{j-1}, t_{j-1}) \\
&\quad \times \Big( (m-j+1)^{\wp+1} - (m-j)^\wp (m-j+1+\wp) \Big) \Big], \\
S_m^{m+1} &= S_m^0 + \frac{\vartheta h^\wp}{\Gamma(\wp+2)} \sum_{j=0}^{m} \Big[ t_j^{\vartheta-1} g_5(S_r^j, V_r^j, I_r^j, R_r^j, S_m^j, I_m^j, t_j) \\
&\quad \times \Big[ (m+1-j)^\wp (m-j+2+\wp) - (m-j)^\wp (m-j+2 \\
&\quad + 2\wp) \Big] - t_{j-1}^{\vartheta-1} g_5(S_r^{j-1}, V_r^{j-1}, I_r^{j-1}, R_r^{j-1}, S_m^{j-1}, I_m^{j-1}, t_{j-1}) \\
&\quad \times \Big( (m-j+1)^{\wp+1} - (m-j)^\wp (m-j+1+\wp) \Big) \Big],
\end{aligned} \quad (4.18)$$

$$
\begin{aligned}
S_m^{m+1} =& S_m^0 + \frac{\vartheta h^{\wp}}{\Gamma(\wp+2)} \sum_{j=0}^{m} \Big[ t_j^{\vartheta-1} g_6(S_r^j, V_r^j, I_r^j, R_r^j, S_m^j, I_m^j, t_j) \\
&\times \Big[ (m+1-j)^{\wp}(m-j+2+\wp) - (m-j)^{\wp}(m-j \\
&+ 2 + 2\wp) \Big] - t_{j-1}^{\vartheta-1} g_6(S_r^{j-1}, V_r^{j-1}, I_r^{j-1}, R_r^{j-1}, S_m^{j-1}, I_m^{j-1}, \\
&t_{j-1}) \times \Big( (m-j+1)^{\wp+1} - (m-j)^{\wp}(m-j+1+\wp) \Big) \Big].
\end{aligned}
$$

### *4.1. Existence and uniqueness analysis*

In this subsection of the paper, we will focus on the existence and uniqueness of the fractal-fractional Caputo derivative. We utilize the result of [53] and take the Cauchy problem with power law as

$$\hbar(t) = \hbar(0) + \frac{\wp\vartheta}{\Gamma(\wp)} \int_0^t \chi^{\vartheta-1} g(\chi, \hbar(\chi)) d\chi. \tag{4.19}$$

Furthermore, we define the map of the form

$$\Phi\theta(t) = \hbar(0) + \frac{\wp\vartheta}{\Gamma(\wp)} \int_0^t \Phi^{\theta-1} g(\Phi, \psi(\chi)) d\chi, \tag{4.20}$$

which implies that

$$\|\Phi\theta(t) - \hbar(0)\| < k \Longrightarrow V, \tag{4.21}$$

where

$$V = \sup_{\Pi_e^c} |g|$$

and

$$V < \frac{k\Gamma(\wp)}{\wp\vartheta c^{\vartheta+\wp-3} B(\vartheta, \wp)}.$$

In the next step, we consider $\theta_1$ and $\theta_2 \in C[I_n(t_n), A_e(t_n)]$, and compute the below inequality

$$\|\Phi\theta_1 - \Phi\theta_2\| < \frac{\wp\vartheta L}{\Gamma(\wp)} c^{\vartheta+\wp-3} B(\vartheta, \wp). \tag{4.22}$$

In consequences, we obtained the contractive property as follows

$$L < \frac{\Gamma(\wp)}{\wp\vartheta c^{\vartheta+\wp-3} B(\vartheta, \wp)}. \tag{4.23}$$

In the case, if the above is obtained then we have

$$V < \frac{k\Gamma(\wp)}{\wp\vartheta c^{\vartheta+\wp-3} B(\vartheta, \wp)}, \tag{4.24}$$

thus, under power law the existence and uniqueness proof for the solution is completed.

### *4.2. Simulation results with discussion*

Modeling approaches are utilized to conceptualize and understand the complex phenomena of the biological process. Several mathematical models have been presented in the literature to visualize the transmission pathway of RVF. In [54], a comprehensive overview of the compartmental model for transmission dynamics of RVF has been presented. It has been noticed that RVF brings unimaginable damage to the economic sectors around the world and effect public health. The authors in [55] formulated a mathematical model with impulsive vaccination to identify the role of pulse vaccination in the control and prevention of the disease. Further, investigation is needed to identify the most critical input factors and investigate the dynamical behavior of RVF for better understanding. In this section, the most important biological parameters are selected to analyze behavior of infected human population $I_r$ of the proposed FF model for the RVF epidemic. Biological parameters of great interest are:the fractal order $\wp$, fractional order $\vartheta$, biting rate of vector mosquitoes $b$, efficacy of vaccine $\alpha$, transmission rate from mosquitoes to susceptible ruminants $\beta_r$, transmission rate from ruminants to susceptible mosquitoes $\beta_m$, recovery rate of infected ruminants $\gamma$, and the recovery through vaccination of ruminants host $\rho$. All parameters have been taken from the above listed Table 1 otherwise stated. These important parameters have been varied in either decreasing to increasing or vice versa way to observe dynamical behavior of the RVF model under FF setting of the Caputo operator. It may also be noted that the simulations in this sections are carried out under the novel numerical scheme developed for the FF Caputo operator as shown in (4.18) above.

As can be observed in Figure 5, the RVF infected population of humans will start to increase if the fractional order $\vartheta$ (with $\wp = 1$) or the fractal order $\wp$ (with $\vartheta = 1$) approach to 1 thereby shows some values of these orders under FF Caputo operator to be between $[0, 1]$. Similarly, if the biting rate of vector mosquitoes $b$ is maintained at relatively some lower level then the infection does not grow as is seen in (a) plot of Figure 6 and this can be achieved if most susceptible people start to use mosquitoes protective nets or some liquid (medicinal or an oil) on exposed parts

of their body while in the plot (b) of the same figure that the improved value of efficacy of vaccine plays some role to lower the infection level.

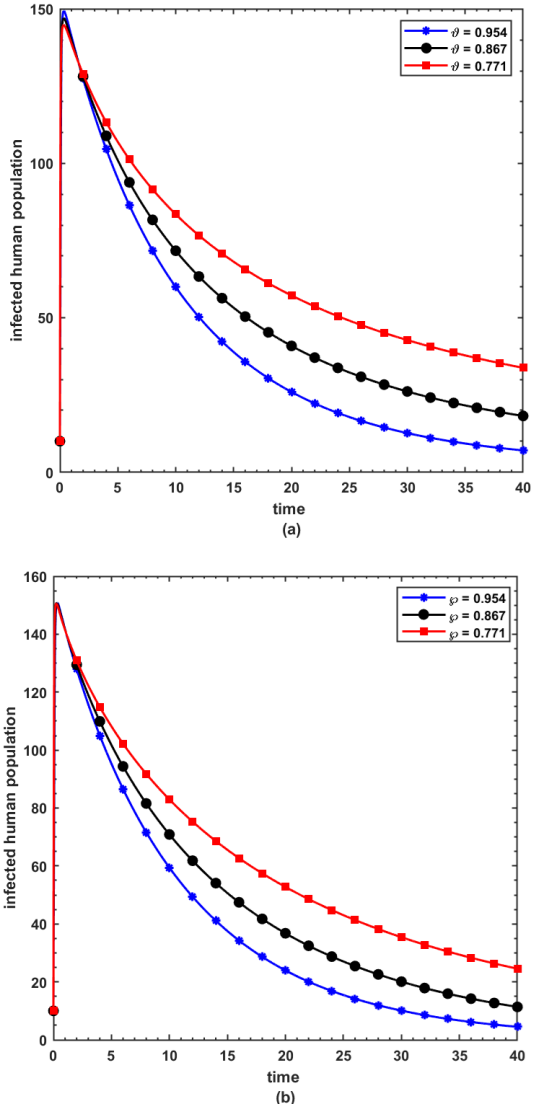


**Figure 5.** Dynamical behavior of infected human population with different values of (a) fractional order $\vartheta$ when $\wp = 1$ and (b) fractal order $\wp$ when $\vartheta = 1$ while remaining parameters have been taken from Table 1.

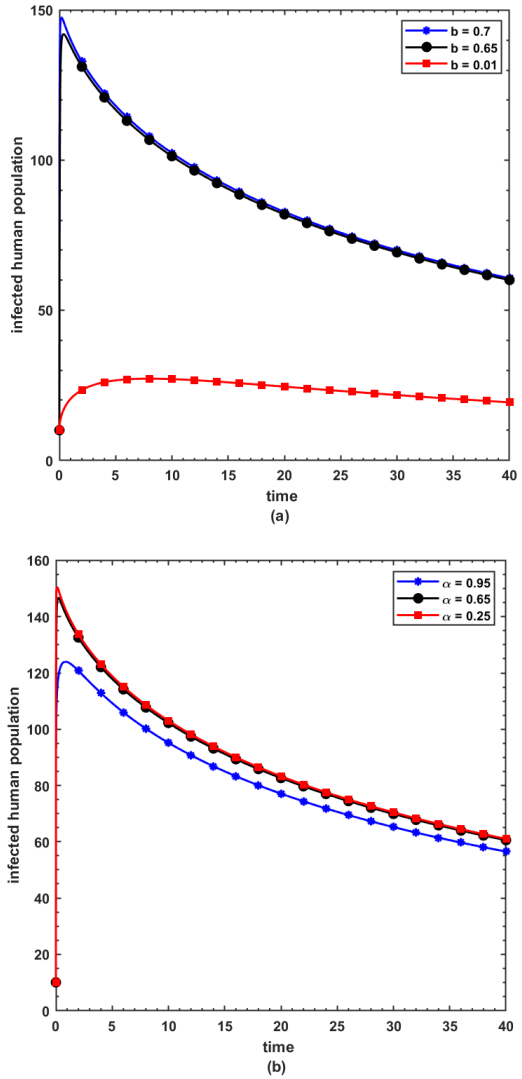


**Figure 6.** Dynamical behavior of infected human population with different values of (a) biting rate of vector mosquitoes $b$ and (b) efficacy of vaccine $\alpha$ while remaining parameters have been taken from Table 1.

Most interestingly, plot (a) of Figure 7 shows that the decreasing transmission rate from mosquitoes to susceptible ruminants $\beta_r$ is more useful than decreasing transmission rate from ruminants to susceptible mosquitoes $\beta_m$ as is observable in (b) plot of the same figure. Finally, it can be observed from plot (a) of the Figure 8 that the recovery rate of infected ruminants $\gamma$ holds significant importance and warrants careful consideration. A small value of $\gamma$ can have devastating consequences. Moreover, plot (b) indicates

that while vaccination can reduce the infection level, its effectiveness may not be optimal under the assumptions of our model. Therefore, alternative effective measures need to be implemented to address the RVF epidemic in the current scenarios.

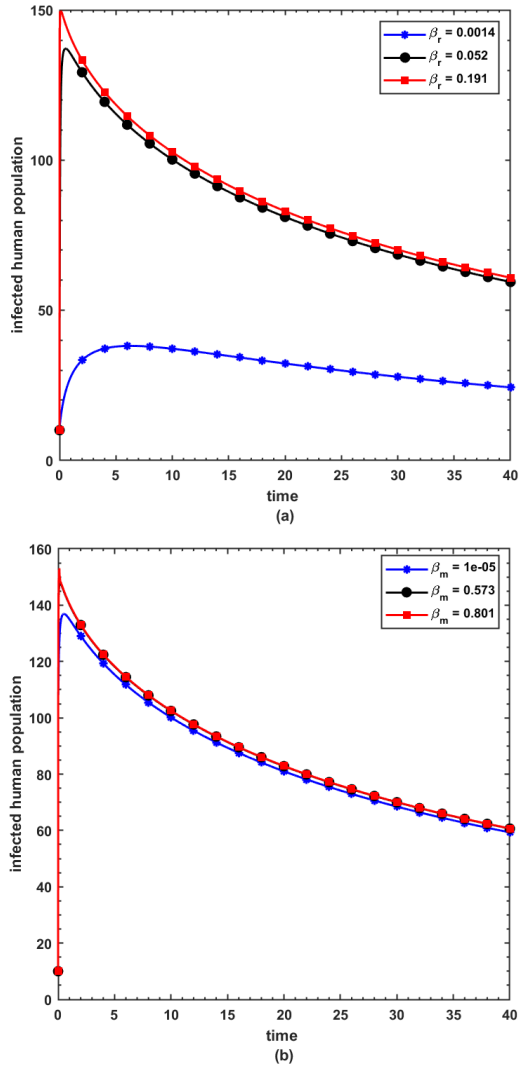


**Figure 7.** Dynamical behavior of infected human population with different values of (a) transmission rate from mosquitoes to susceptible ruminants $\beta_r$ and (b) transmission rate from ruminants to susceptible mosquitoes $\beta_m$ while remaining parameters have been taken from the Table 1.

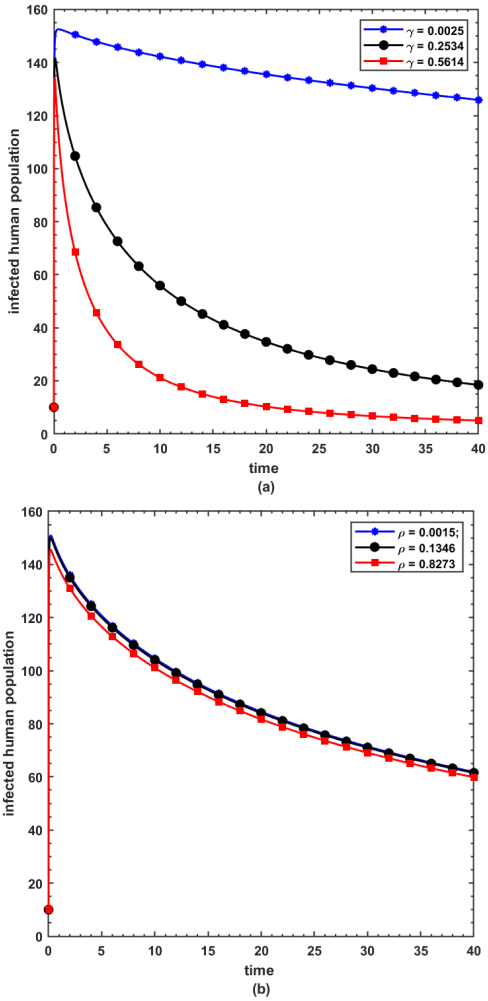


**Figure 8.** Dynamical behavior of infected human population with different values of (a) recovery rate of infected ruminants $\gamma$ and (b) recovery through vaccination of ruminants host $\rho$ while remaining parameters have been taken from the Table 1.

## 5. Conclusions

It is evident that the infection of the RVF virus poses a significant threat to the economic sector. Therefore, it is valuable to visualize the transmission pathway of this vector-borne infection and to point out the critical factor that greatly disturb the dynamics of the infection. In this research article, we formulated a fractal-fractional model for the transmission of RVF in ruminant host in the Caputo's framework to study the intricate system of the infection.

First, we presented the rudimentary knowledge of fractal-fractional derivative for analysis of the proposed system. The model is then investigated for some basic results and then we determined the basic reproduction number through the next-generation matrix technique, indicated by $\mathcal{R}_0$. The PRCC technique is utilized to interrogate the global sensitivity of reproduction parameter $\mathcal{R}_0$ to find out the most sensitive input-factors to the basic reproduction number $\mathcal{R}_0$. In this research, we established the existence and uniqueness results of the proposed fractal-fractional model. Furthermore, we presented the fractal-fractional dynamics of the proposed RVF model through a novel numerical scheme. In the end, the proposed fractal-fractional system of RVF is visualized numerically with different values of fractal/fractional orders and other input parameters for the control of RVF. Our analysis indicates that these parameters have the potential to significantly reduce the infection level and can play a crucial role in the control and prevention of the disease.

## Use of AI tools declaration

The authors declare that they have not used Artificial Intelligence tools in the creation of this article.

## Conflict of interest

The authors declare that there are no conflicts of interest in this paper.

## References


1. R. Daubney, J. R. Hudson, Enzootic hepatitis or Rift Valley fever, an un-described virus disease of sheep, cattle and man from East Africa, *J. Pathol. Bacteriol.*, **34** (1931), 545–579. https://doi.org/10.1002/path.1700340418
2. S. Abdo-Salem, A. Tran, V. Grosbois, G. Gerbier, M. Al-Qadasi, K. Saeed, et al., Can environmental and socioeconomic factors explain the recent emergence of Rift Valley fever in Yemen, 2000-2001? *Vector Borne Zoonot. Dis.*, **11** (2011), 773–779. https://doi.org/10.1089/vbz.2010.0084
3. C. A. Mebus, Rift Valley fever, *Access Sci.*, 2014. https://doi.org/10.1036/1097-8542.757367
4. A. Anyamba, J. P. Chretien, J. Small, C. J. Tucker, P. B. Formenty, J. H. Richardson, et al., Prediction of a Rift Valley fever outbreak, *Proc. Natl. Acad. Sci.*, **106** (2009), 955–959. https://doi.org/10.1073/pnas.0806490106
5. N. Chitnis, J. M. Hyman, C. A. Manore, Modelling vertical transmission in vector-borne diseases with applications to Rift Valley fever, *J. Biol. Dyn.*, **7** (2013), 11–40. https://doi.org/10.1080/17513758.2012.733427
6. S. Sankhe, C. Talla, M. S. Thiam, M. Faye, M. A. Barry, M. Diarra, et al., Seroprevalence of Crimean-Congo Hemorrhagic Fever virus and Rift Valley fever virus in human population in Senegal from October to November 2020, *IJID Regions*, **7** (2023), 216–221. https://doi.org/10.1016/j.ijregi.2023.03.016
7. M. K.Trabelsi, A. Hachid, F. Derrar, N. E. Messahel, T. Bia, Y. Mockbel, et al., Serological evidence of Rift Valley fever viral infection among camels imported into Southern Algeria, *Comp. Immunol. Microbiol. Infect. Dis.*, **100** (2023), 102035. https://doi.org/10.1016/j.cimid.2023.102035
8. S. C. Mpeshe, H. Haario, J. M. Tchuenche, A mathematical model of Rift Valley fever with human host, *Acta Biotheor.*, **59** (2011), 231–250. https://doi.org/10.1007/s10441-011-9132-2
9. J. K. Gitau, R. W. Macharia, K. W. Mwangi, N. Ongeso, E. Murungi, Gene co-expression network identifies critical genes, pathways and regulatory motifs mediating the progression of rift valley fever in Bos taurus, *Heliyon*, **9** (2023), e18175. https://doi.org/10.1016/j.heliyon.2023.e18175
10. L. Xue, H. M. Scott, L. W. Cohnstaedt, C. Scoglio, A network-based meta-population approach to model Rift Valley fever epidemics, *J. Theor. Biol.*, **306** (2012), 129–144. https://doi.org/ 10.1016/j.jtbi.2012.04.029
11. D. Gao, C. Cosner, R. S. Cantrell, J. C. Beier, S. Ruan, Modeling the spatial spread of Rift Valley fever in Egypt, *Bullt. Math. Biol.*, **75** (2013), 523–542. https://doi.org/10.1007/s11538-013-9818-5

12. C. Catre-Sossah, C. Lebon, P. Rabarison, E. Cardinale, P. Mavingui, C. Atyame, Evidence of Eretmapodites subsimplicipes and Aedes albopictus as competent vectors for Rift Valley fever virus transmission in Mayotte, *Acta Trop.*, **239** (2023), 106835. https://doi.org/10.1016/j.actatropica.2023.106835

13. R. Jan, Y. Xiao, Effect of partial immunity on transmission dynamics of dengue disease with optimal control, *Math. Methods Appl. Sci.*, **42** (2019), 1967–1983. https://doi.org/10.1002/mma.5491

14. N. N. H. Shah, R. Jan, H. Ahmad, N. N. A. Razak, I. Ahmad, H. Ahmad, Enhancing public health strategies for tungiasis: a mathematical approach with fractional derivative, *AIMS Bioeng.*, **10** (2023), 384–405. https://doi.org/10.3934/bioeng.2023023

15. R. Jan, Y. Xiao, Effect of pulse vaccination on dynamics of dengue with periodic transmission functions, *Adv. Differ. Equations*, **2019** (2019), 368. https://doi.org/10.1186/s13662-019-2314-y

16. T. Ikegami, S. Makino, Rift valley fever vaccines, *Vaccine*, **27** (2009), 69–72. https://doi.org/10.1016/j.vaccine.2009.07.046

17. G. F. Ronchi, L. Testa, M. Iorio, C. Pinoni, G. Bortone, A. C. Dondona, et al., Immunogenicity and safety studies of an inactivated vaccine against Rift Valley fever, *Acta Trop.*, **232** (2022), 106498. https://doi.org/10.1016/j.actatropica.2022.106498

18. J. C. Morrill, C. J. Peters, G. E. Bettinger, P. M. Palermo, D. R. Smith, D. M. Watts, Rift Valley fever MP-12 vaccine elicits an early protective immune response in mice, *Vaccine*, **40** (2022), 7255–7261. https://doi.org/10.1016/j.vaccine.2022.10.062

19. F. Chamchod, R. S. Cantrell, C. Cosner, A. N. Hassan, J. C. Beier, S. Ruan, A modeling approach to investigate epizootic outbreaks and enzootic maintenance of Rift Valley fever virus, *Bull. Math. Biol.*, **76** (2014), 2052–2072. https://doi.org/10.1007/s11538-014-9998-7

20. I. Ahmad, M. Ahsan, I. Hussain, P. Kumam, W. Kumam, Numerical simulation of PDEs by local meshless differential quadrature collocation method, *Symmetry*, **11** (2019), 394. https://doi.org/10.3390/sym11030394

21. M. N. Khan, I. Ahmad, M. Shakeel, R. Jan, Fractional calculus analysis: investigating Drinfeld-Sokolov-Wilson system and Harry Dym equations via meshless procedures, *Math. Model. Control*, **4** (2024), 86–100. https://doi.org/10.3934/mmc.2024008

22. M. Shakeel, M. N. Khan, I. Ahmad, H. Ahmad, N. Jarasthitikulchai, W. Sudsutad, Local meshless collocation scheme for numerical simulation of space fractional PDE, *Therm. Sci.*, **27** (2023), 101–109. https://doi.org/10.2298/TSCI23S1101S

23. F. Wang, J. Zhang, I. Ahmad, A. Farooq, H. Ahmad, A novel meshfree strategy for a viscous wave equation with variable coefficients, *Front. Phys.*, **9** (2021), 701512. https://doi.org/10.3389/fphy.2021.701512

24. I. Ahmad, I. Ali, R. Jan, S. A. Idris, M. Mousa, Solutions of a three-dimensional multi-term fractional anomalous solute transport model for contamination in groundwater, *Plos One*, **18** (2023), e0294348. https://doi.org/10.1371/journal.pone.0294348

25. F. Wang, I. Ahmad, H. Ahmad, M. D. Alsulami, K. S. Alimgeer, C. Cesarano, et al., Meshless method based on RBFs for solving three-dimensional multi-term time fractional PDEs arising in engineering phenomenons, *J. King Saud Univ.*, **33** (2021), 101604. https://doi.org/10.1016/j.jksus.2021.101604

26. I. Ahmad, H. Ahmad, A. E. Abouelregal, P. Thounthong, M. Abdel-Aty, Numerical study of integer-order hyperbolic telegraph model arising in physical and related sciences, *Eur. Phys. J. Plus*, **135** (2020), 759. https://doi.org/10.1140/epjp/s13360-020-00784-z

27. Z. U. Rehman, S. Boulaaras, R. Jan, I. Ahmad, S. Bahramand, Computational analysis of financial system through non-integer derivative, *J. Comput. Sci.*, **75** (2024), 102204. https://doi.org/10.1016/j.jocs.2023.102204

28. H. Ahmad, M. N. Khan, I. Ahmad, M. Omri, M. F. Alotaibi, A meshless method for numerical solutions of linear and nonlinear time-fractional Black-Scholes models, *AIMS Math.*, **8** (2023), 19677–19698. https://doi.org/ 10.3934/math.20231003

29. I. Ahmad, A. A. Bakar, I. Ali, S. Haq, S. Yussof, A. H. Ali, Computational analysis of time-fractional models in energy infrastructure applications, *Alex. Eng. J.*, **82** (2023), 426–436. https://doi.org/10.1016/j.aej.2023.09.057

30. Z. Shah, E. Bonyah, E. Alzahrani, R. Jan, N. A. Alreshidi, Chaotic phenomena and oscillations in dynamical behaviour of financial system via fractional calculus, *Complexity*, **2022** (2022), 8113760. https://doi.org/10.1155/2022/8113760

31. W. Deebani, R. Jan, Z. Shah, N. Vrinceanu, M. Racheriu, Modeling the transmission phenomena of water-borne disease with non-singular and non-local kernel, *Comput. Methods Biomech. Biomed. Eng.*, **26** (2022), 1294–1307. https://doi.org/10.1080/10255842.2022.2114793

32. M. Farman, H. Besbes, K. S. Nisar, M. Omri, Analysis and dynamical transmission of Covid-19 model by using Caputo-Fabrizio derivative, *Alex. Eng. J.*, **66** (2023), 597–606. https://doi.org/10.1016/j.aej.2022.12.026

33. J. Li, I. Ahmad, H. Ahmad, D. Shah, Y. M. Chu, P. Thounthong, et al., Numerical solution of two-term time-fractional PDE models arising in mathematical physics using local meshless method, *Open Phys.*, **18** (2020), 1063–1072. https://doi.org/10.1515/phys-2020-0222

34. I. Ahmad, M. Riaz, M. Ayaz, M. Arif, S. Islam, P. Kumam, Numerical simulation of partial differential equations via local meshless method, *Symmetry*, **11** (2019), 257. https://doi.org/10.3390/sym11020257

35. K. S. Nisar, M. Farman, E. Hincal, A. Shehzad, Modelling and analysis of bad impact of smoking in society with Constant Proportional-Caputo Fabrizio operator, *Chaos Solitons Fract.*, **172** (2023), 113549. https://doi.org/10.1016/j.chaos.2023.113549

36. A. Atangana, J. J. Nieto, Numerical solution for the model of RLC circuit via the fractional derivative without singular kernel, *Adv. Mech. Eng.*, **7** (2015), 1687814015613758. https://doi.org/10.1177/1687814015613758

37. H. M. Srivastava, R. Jan, A. Jan, W. Deebani, M. Shutaywi, Fractional-calculus analysis of the transmission dynamics of the dengue infection, *Chaos*, **31** (2021), 053130. https://doi.org/10.1063/5.0050452

38. S. Qureshi, A. Yusuf, Fractional derivatives applied to MSEIR problems: comparative study with real world data, *Eur. Phys. J. Plus*, **134** (2019), 171. https://doi.org/10.1140/epjp/i2019-12661-7

39. T. Q. Tang, Z. Shah, R. Jan, W. Deebani, M. Shutaywi, A robust study to conceptualize the interactions of $CD4^+$ T-cells and human immunodeficiency virus via fractional-calculus, *Phys. Scr.*, **96** (2021), 125231. https://doi.org/10.1088/1402-4896/ac2d7b

40. O. M. Ogunmiloro, A fractional order mathematical model of teenage pregnancy problems and rehabilitation in Nigeria, *Math. Modell. Control*, **2** (2022), 139–152. https://doi.org/10.3934/mmc.2022015

41. M. Caputo, Linear models of dissipation whose Q is almost frequency independent-II, *Geophys. J. Int.*, **13** (1967), 529–539. https://doi.org/10.1111/j.1365-246X.1967.tb02303.x

42. K. S. Nisar, M. Farman, M. Abdel-Aty, J. Cao, A review on epidemic models in sight of fractional calculus, *Alex. Eng. J.*, **75** (2023), 81–113. https://doi.org/10.1016/j.aej.2023.05.071

43. Z. Li, Z. Liu, M. A. Khan, Fractional investigation of bank data with fractal-fractional Caputo derivative, *Chaos Solitons Fract.*, **131** (2020), 109528. https://doi.org/10.1016/j.chaos.2019.109528

44. M. Farman, S. Jamil, K. S. Nisar, A. Akgul, Mathematical study of fractal-fractional leptospirosis disease in human and rodent populations dynamical transmission, *Ain Shams Eng. J.*, **15** (2023), 102452. https://doi.org/10.1016/j.asej.2023.102452

45. J. A. P. Heesterbeek, A brief history of R0 and a recipe for its calculation, *Acta Biotheor.*, **50** (2002), 189–204. https://doi.org/10.1023/a:1016599411804

46. J. Yangla, H. Abboubakar, E. Dangbe, R. Yankoulo, A. A. A. Ari, I. Damakoa, et al., Fractional dynamics of a Chikungunya transmission model, *Sci. Afr.*, **21** (2023), e01812. https://doi.org/10.1016/j.sciaf.2023.e01812

47. K. N. Nabi, H. Abboubakar, P. Kumar, Forecasting of Covid-19 pandemic: from integer derivatives to fractional derivatives, *Chaos Solitons Fract.*, **141** (2020), 110283. https://doi.org/10.1016/j.chaos.2020.110283

48. S. Marino, I. B. Hogue, C. J. Ray, D. Kirschner, A methodolojgy for performing global uncertainty and sensitivity analysis in systems biology, *J. Theor. Biol.*, **254** (2008), 178–196. https://doi.org/10.1016/j.jtbi.2008.04.011

49. A. A. Majok, K. H. Zessin, M. P. O. Baumann, T. B. Farver, Analyses of baseline survey data on rinderpest in Bahr el Ghazal Province, with proposal of an improved vaccination strategy against rinderpest for southern Sudan, *Trop. Anim. Health Prod.*, **23** (1991), 186–196. https://doi.org/10.1007/BF02357004

50. D. V. Canyon, J. L. K Hii, R. Muller, The frequency of host biting and its effect on oviposition and survival in Aedes aegypti (Diptera: Culicidae), *Bull. Entomol. Res.*, **89** (1999), 35–39. https://doi.org/10.1017/S000748539900005X

51. M. J. Turell, K. J. Linthicum, L. A. Patrican, F. G. Davies, A. Kairo, C. L. Bailey, Vector competence of selected African mosquito (Diptera: Culicidae) species for Rift Valley fever virus, *J. Med. Entomol.*, **45** (2008), 102–108. https://doi.org/10.1093/jmedent/45.1.102

52. M. H. Reiskind, C. J. Westbrook, L. P. Lounibos, Exposure to chikungunya virus and adult longevity in Aedes aegypti (L.) and Aedes albopictus (Skuse), *J. Vector Ecol.*, **35** (2010), 61–68. https://doi.org/10.1111/j.1948-7134.2010.00059.x

53. A. Atangana, Q. Sania, Modeling attractors of chaotic dynamical systems with fractal-fractional operators, *Chaos Solitons Fract.*, **123** (2019), 320–337. https://doi.org/10.1016/j.chaos.2019.04.020

54. M. L. Danzetta, R. Bruno, F. Sauro, L. Savini, P. Calistri, Rift Valley fever transmission dynamics described by compartmental models, *Prev. Vet. Med.*, **134** (2016), 197–210. https://doi.org/10.1016/j.prevetmed.2016.09.007

55. C. Yang, L. Nie, Modelling the use of impulsive vaccination to control Rift Valley fever virus transmission, *Adv. Differ. Equations*, **2016** (2016), 134. https://doi.org/10.1186/s13662-016-0835-1


AIMS Press